Plasma Generation with a Resonant Planar Antenna

Ph. Guittienne, HELYSSEN Sa`rl, Belmont-sur-Lausanne, Switzerland; P. Fayet and J. Larrieu, Tetra Pak (Suisse) SA, D&E, Advanced Film and Barrier Solutions, Romont, Switzerland; and A.A. Howling and Ch. Hollenstein, Centre de Recherches en Physique des Plasmas, Lausanne, Switzerland

ABSTRACT

A planar RF antenna is presented for potential plasma processing applications. It consists of an arrangement of elementary resonant meshes which presents a set of resonant modes, *i.e.* resonant frequencies. When excited at one of these frequencies the antenna develops a strong sinusoidal current distribution. A rectangular RF (13.56 MHz) plasma source with a 0.2m×0.55m antenna has been built and electron densities of about 4.10^{11} cm^{-3} have been measured by 33 GHz interferometry at a distance of 4 cm from the source plane for an injected RF power of 2000 kW. The discharge was shown to be driven by inductive coupling with the resonant current distribution of the antenna. For an operating pressure of 5 Pa the plasma non-uniformity was less than ±5% over 75% of the antenna surface. Besides its high efficiency for plasma generation, this antenna has the key advantage of being theoretically scalable up to very large surfaces without presenting the usual limitations in terms of RF power injection and of impedance matching met by conventional large area plasma sources.

INTRODUCTION

In this paper we present the principles of a resonant RF (radio frequency) planar antenna (HELYSSEN antenna) suitable for both large area processing and high electron density. Large area plasma processing [1–3] (typically over 1 m^2) is particularly interesting for developing new products in domains such as large area flat panel displays, packaging, and thin film solar cells. Even for wafer based processes, large area processing will allow much larger amounts of pieces to be treated at the same time, thus increasing the production throughput. Conventional large area RF sources (inductively or capacitively coupled) suffer notably from the fact that their input impedance is almost purely reactive and tends toward critical values (zero or infinity) with increasing process area. On the contrary the resonant network presented here exhibits a real and peaked input impedance which makes the injection of the RF power much easier. These impedance properties are shown to be independent of the antenna dimensions. A small plasma source of 55 cm by 20 cm has been built and tested on a pilot line roll-to-roll installation for barrier thin film deposition in comparison with standard magnetron sources. The HELYSSEN antenna was shown to be much more efficient in terms of process rate for equivalent barrier properties of the deposited films.

PRINCIPLES OF THE HELYSSEN PLANAR ANTENNA

The present section describes briefly the principles of the HELYSSEN planar antenna [4, 5]. Its structure and operating principles are similar to the closed cylindrical birdcage antenna previously described [6, 7] but it has been unwrapped to form an open and planar structure as shown in Figure 1.

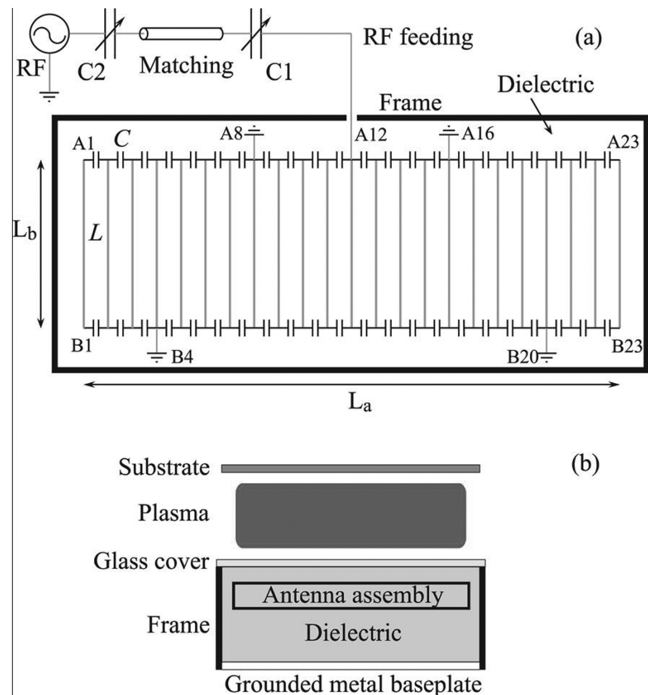

Figure 1: (a) Schematic top view of the planar RF antenna showing the antenna bars (inductance L), the capacitors (C), and the matching network. (b) Schematic end view of the antenna showing the grounded metal baseplate, the metal frame sidewalls, and the antenna embedded in the dielectric with a protective glass cover. A substrate can be placed above the plasma as shown. The whole assembly is placed within the vacuum vessel.

The planar antenna is suited for large area surface treatment, whereas the cylindrical version is adapted to plasma processes requiring a volume plasma source. In both cases, the ***N*** parallel legs of the antenna are made of copper tubes which can be taken to act essentially as inductive elements of inductance ***L***. High Q capacitors of capacitance ***C*** link the legs together

© **2012 Society of Vacuum Coaters** 505/856-7188

55th Annual Technical Conference Proceedings, Santa Clara, CA April 28–May 3, 2012 ISSN 0737-5921

and present also a small inductance M formed by the metallic leads. In the framework of a lumped elements analysis, and considering the ideal non-dissipative case, the impedance of the legs, and the impedance of segments containing a capacitor are purely imaginary. Solving the Kirchhoff equations over the antenna with the open boundary conditions of the planar structure gives N-1 resonant modes m that arise from the parallel assembly of L and C components. Each of these modes is characterized by a resonance frequency f_m and by specific current distributions in each segment I_n, M_n, and K_n and voltage distributions at the nodes A_n and B_n. The resonance frequencies are given by (eq. 1):

$$\omega_m = 2\pi \cdot f_m = \left[C\left(M - 2L\sin^2\left\{\frac{m\pi}{2N}\right\}\right)\right]^{-\frac{1}{2}} \tag{1}$$

Assuming that the antenna is excited at one of its resonance frequencies by an excitation potential $V_{in} = V_0.\cos(\omega t)$ at the feeding node A_{Nf} and grounded at node A_{Ng}, the expressions for the leg currents I_n and capacitor currents M_n and K_n simplify to:

$$\begin{cases} I_n = \dfrac{2V_0}{DL\omega_m} \cdot \cos\{k_m(2n-1)\}\sin\{\omega_m t\} \\ M_n = -K_n = \dfrac{V_0}{DL\omega_m \sin\{k_m\}}\sin\{2k_m n\}\sin\{\omega_m t\} \end{cases} \tag{2}$$

$$\begin{cases} A_n = \dfrac{V_0}{D} \cdot \left[\cos\{k_m(2n-1)\} - \cos\{k_m(2N_g-1)\}\right]\cos\{\omega_m t\} \\ B_n = -\dfrac{V_0}{D} \cdot V_0\left[\cos\{k_m(2n-1)\} + \cos\{k_m(2N_g-1)\}\right]\cos\{\omega_m t\} \end{cases} \tag{3}$$

with $D = \cos\{k_m(2N_f-1)\} - \cos\{k_m(2N_g-1)\}$ and $k_m = \dfrac{m\pi}{2N}$.

Note that these equations all have sinusoidal forms and oscillate temporally in phase. The spatial wavelength is inversely proportional to the mode number m. For instance, three normalized distributions are shown in Figure 2 corresponding to the modes $m = 1$, $m = 2$, and $m = 6$ for a 23-leg antenna. Note that the current intensities in the legs for the $m = 1$ mode constitute a half wavelength over the antenna length, while three wavelengths occur for the mode $m = 6$.

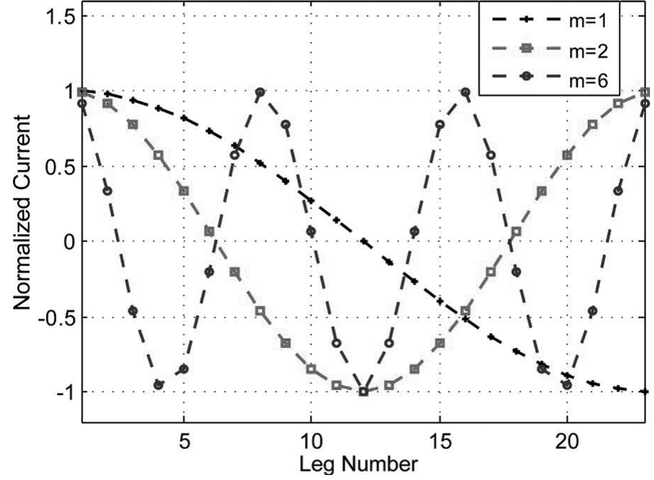

Figure 2: Current distributions in the conductive legs for different modes of a 23-leg RF antenna. The symbols indicate the currents in each leg; the lines show the mode structure.

EXPERIMENTAL RESULTS

The results presented below have been obtained with a small planar source (55 by 20 cm) operated at 13.56 MHz. The $m = 6$ resonance of the system has been brought to this industrial frequency by adjusting the value of the antenna capacitors (2.9 nF). The antenna was shown to couple inductively to the plasma for an injected RF power of about 50-100W, depending on the operating pressure (typ. 10^{-3} to 10^{-1} mbar). The transition between capacitive and inductive couplings can be observed as a jump in the measurement (33GHz interferometry) of the electron density during a power ramp (Figure 3). The plasma density reaches values of about 10^{11} cm^{-3} for 1 kW of power injection, and no saturation is observed in the 2 kW range of our experiment.

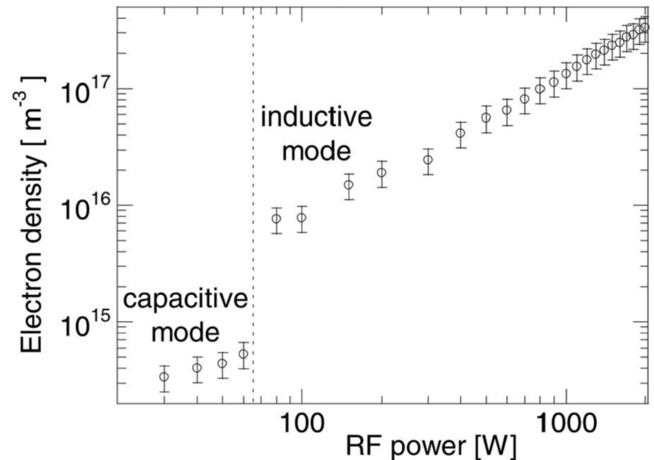

Figure 3: Maximum electron density measured by 33 GHz interferometer in the Ar plasma for increasing RF power going from 30W to 2000W. The Ar pressure is 10^{-2} mbar, and the flux is 30 sccm. The transition from capacitive to inductive coupling occurs at around 60W.

The electron density along the middle of the antenna is given in Figure 4. These profiles broaden with increasing power from 100W to 200W and finally to 1000W. Black marks indicate the position of the legs with maximal currents and correspond effectively to the local maxima of density. Notice how the two electron density maxima located near the edges of the antenna at ±20 cm are progressively raised to the same values as the three maxima located near the central feeding, showing that the plasma becomes more and more uniform with increasing power. This indicates that the plasma ionization rate begins to dominate the diffusion loss process at the edges and extend the high electron density from the centre of the antenna to the edges resulting in only 65% non-uniformity over more than 75% of the antenna at 1000W.

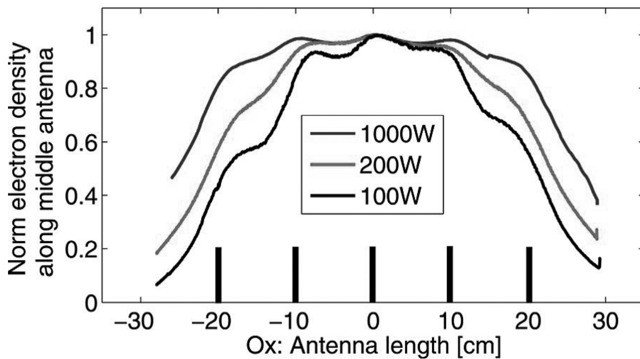

Figure 4: Electron density profiles (normalized) along the RF antenna length at 100, 200, and 1000W at a distance of 4 cm above the antenna. The black line segments indicate the positions of the legs with maximal currents.

The planar plasma source has been installed in a pilot roll-to-roll semi-industrial installation (Tetra Pak) in order to test its performances in comparison with conventional magnetron sources. Thin barrier films (typ. 20 nm) have been deposited on pet foils (50 cm width) at different line speeds, and the quality of the obtained barrier was characterized by measuring the oxygen and water transmission rates across the processed substrates. The conventional magnetron process allows good barriers to be reached with a line speed of about 10 m/min, with an injected 40 kHz power of typically 2 kW. With the HELYSSEN source, good barriers were obtained at the maximum available speed of the pilot line (40 m/min) for a RF power of 1.3 kW. On the basis of the deposition rate (65 nm/s) reached with the resonant network, the line speed could even be raised up to 60 m/min.

PERSPECTIVES

The experimental results obtained with the HELYSSEN planar source are very promising. It has been shown that the high efficiency of the resonant network in terms of plasma density allows high process rates to be reached. In addition we show in this section that the resonant network is also theoretically an excellent candidate to produce very large area plasma sources.

One of the recurrent difficulties in the attempt to increase the area of conventional RF plasma sources lies in the input impedance ($\boldsymbol{Z}_{in}$) problem. Taking a capacitively coupled source, its input impedance will drop zero with increasing area. On the contrary the input impedance (essentially reactive) of a conventional inductively coupled source, such as a spiral antenna, will tend toward infinity with the antenna size. These critical values of $\boldsymbol{Z}_{in}$ make the impedance matching between the RF generator and the plasma source very difficult and lead to very high currents/voltages into the feeding lines, which cause destructive arcing and overheating.

Under resonance the HELYSSEN antenna presents a peaked real input impedance (Figure 5). When coupled with the plasma this real input impedance is typically of few tens of ohms, which means that the system is almost already matched and then all the problems mentioned with the input impedance of conventional sources are avoided. The striking point is that these properties are not dependent on the antenna size, at least theoretically.

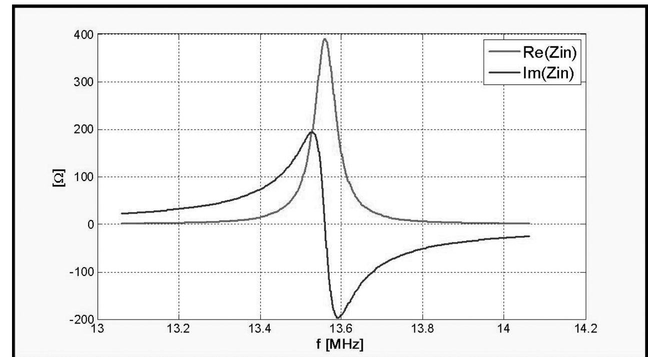

Figure 5: Input impedance of the resonant antenna in the vicinity of the 13.56 MHz m = 6 resonance (without plasma).

Another point concerns the standing wave effect that currently occurs in large area systems. By introducing an electromagnetic model for the antenna conductors instead of the conventional lumped elements analysis, Kirchhoff equations can be solved by taking into account the amplitude variations of the voltages and currents along the conductors. The first very important result of this model is that no relevant standing wave effect is to be expected in the direction perpendicular to the antenna legs. This is due to the fact that the relevant length scale for the standing waves in this direction is not the full antenna length but rather the size of one segment containing a capacitor, which is always much smaller than the potential/current wavelength at our operating frequencies.

Then, standing waves are expected to appear only along the antenna legs. Figure 6 shows a calculation of the currents distribution along 4 meters long legs in an antenna excited at 13.56 MHz (mode ***m* = 6**). It can be seen that a variation of 25% is expected to appear between the middle and the edges of the legs. But the HELYSSEN antenna allows this effect to be easily minimized by introducing a well chosen capacitor in the middle of the legs. The standing wave is then divided and the current amplitude variation is reduced to 8% with no severe reduction of the mean current amplitude.

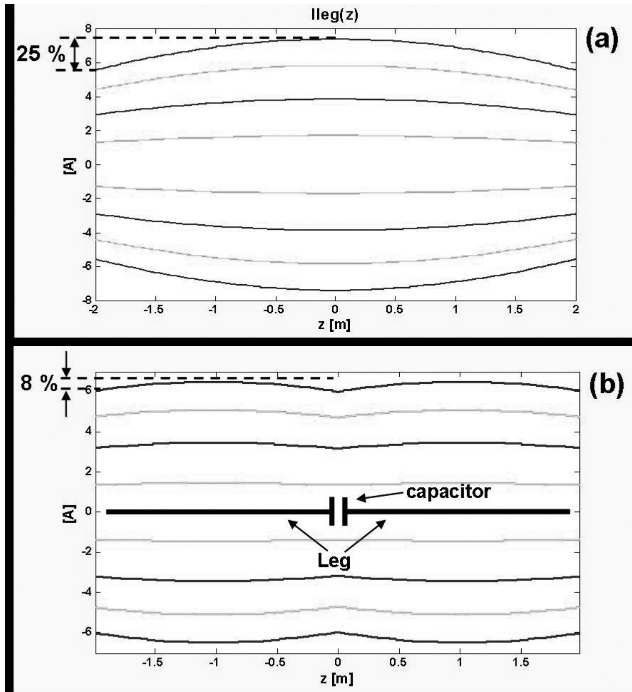

Figure 6: Calculation of the standing wave in a 4 meters long leg. The different lines represent the currents in different legs of the antenna at a given time. Frequency :13.56 MHz. (b) Same calculation with a capacitor (100 pF) inserted in the middle of each leg.

CONCLUSIONS

A prototype of a HELYSSEN planar RF antenna operating at 13.56 MHz has been built and tested up to an RF power of 2000W. The antenna itself constitutes a resonant structure for which the RF voltages and currents have been completely defined theoretically and measured experimentally with an excellent agreement. Argon plasmas are easily ignited and couple inductively above a threshold power of about 60W. The plasma density profiles follow exactly the current distribution corresponding to the mode chosen for excitation, which in this case was the mode m = 6. A plasma non uniformity of less than 5% in terms of electron density was measured at a few centimeters from the antenna. Electron densities above 10^{11} cm^{-3} were measured by microwave interferometry at RF power above 1 kW. In comparison with a conventional 40 kHz magnetron system, the HELYSSEN antenna leads to much higher deposition rates for similar power injection, while the desired barrier properties are preserved. The theoretical analysis of the resonant networks shows that these devices are particularly well adapted to the development of very large area plasma sources, mainly because of their input impedance properties, but also because the standing wave effects can be managed up to very large process areas.

REFERENCES

1. M.A. Lieberman and A.J. Lichtenberg, Principles of Plasma Discharges and Materials Processing (Wiley-Interscience, 2005).

2. H. Chatham, Surf. Coat. Technol. 78, 1 (1996).

3. F.F. Chen, Lecture Notes on Principles of Plasma Processing (Kluwer, 2003).

4. P. Guittienne, see http://www.sumobrain.com/patents/WO2010092433.html for Apparatus for large area plasma processing (August 2010).

5. S. Lecoultre, Ph. Guittienne, A.A. Howling, P. Fayet, and Ch. Hollenstein, J. Phys. D: Appl. Phys. 45, 082001 (2012).

6. J. Jin, Electromagnetic Analysis and Designs in Magnetic Resonance Imaging (CRC, 1998).

7. P. Guittienne and E. Chevalier, J. Appl. Phys. 98, 083304 (2005).